Inorganic Chemistry

Communication

pubs.acs.org/IC

Fabrication of Ruthenium Metal Nanosheets via Topotactic Metallization of Exfoliated Ruthenate Nanosheets

Katsutoshi Fukuda,*[,†] Jun Sato,[‡] Takahiro Saida,[‡] Wataru Sugimoto,*[,‡] Yasuo Ebina,[†] Tatsuo Shibata,[†] Minoru Osada,[†] and Takayoshi Sasaki[†]

[†]International Center for Materials Nanoarchitectonics (MANA), National Institute for Materials Science, 1-1 Namiki, Tsukuba, Ibaraki 305-0044, Japan

[‡]Faculty of Textile Science and Technology, Shinshu University, 3-15-1 Tokida, Ueda, Nagano 386-8567, Japan

Supporting Information

ABSTRACT: The metallization behavior of molecularly thin RuO_2 nanosheets obtained from complete delamination of layered ruthenates was studied. Interestingly, the RuO_2 nanosheets in a monolayer state topotactically transformed into a single layer of Ru atoms, i.e., ruthenium metal nanosheets, which can be regarded as a new family of nanosized metals.

Nanosized metals such as nanoparticles, nanorods, and nanowires have been extensively studied in science and technology.[1] Because they often offer intriguing physical and chemical properties associated with their size and shape on a nanometer scale, it is of essential importance to develop metallic nanomaterials with unique structure and dimension for many applications including electronic, optic, and magnetic devices as well as catalysis.

The so-called "exfoliation technique", in which layered compounds such as clays,[2] oxides,[3] and graphite oxide,[4] are delaminated into elemental host layers, is an emerging state-of-the-art technology that allows two-dimensional (2D) control of nanomaterials. Resulting unilamellar sheets, nanosheets, are characterized by thicknesses of less than several nanometers and lateral sizes in the micrometer regime, thereby offering a unique class of 2D nanocrystallites. Owing to their polyelectrolytic nature, nanosheets can be employed as building blocks for electrostatic self-assembly, utilizing oppositely charged ions, polymers, and molecules. Such artificial nanoarchitectures cannot be easily attained by conventional solid-state reaction and, in some cases, give rise to unique thermodynamic reactivity. For instance, it has been demonstrated that heating ultrathin films of lepidocrocite-related $Ti_{0.91}O_2$ nanosheets yielded anatase thin films with 2D anisotropic crystallites having *c*-axis orientation.[5] This crystallization behavior is highly dependent on the number of deposited nanosheet layers, indicating that both nucleation and growth of anatase from the nanosheet film should require extensive thermal activation of atomic diffusion. More recently, the reduction of exfoliated graphite oxide nanosheets has been shown to yield distinct graphitic structures including graphene, which can be considered as a series of versatile carbon nanomaterials.[4b] Conversion of exfoliated nanosheets or their composites is expected to pave the way to the creation of novel anisotropic nanomaterials.

Ruthenium oxides are promising materials for electronics and energy-related applications because they have a number of attractive properties atypical of most oxide systems, e.g., metallic conductivity.[6] In applications associated with microelectronics, the viability of a RuO_2 thin film to be reduced to ruthenium under a reducing atmosphere has been taken as a concern.[7] This phenomenon motivated us to investigate the conversion of layered ruthenate and its nanosheet derivative[8] to metallic ruthenium. In this study, we report the structural transformation of 2D ruthenates and highlight that the nanosheet in a monolayer state could be topotactically converted into ultimately thin, single-monolayer metal nanosheets.

First, we considered the reduction of a bulk layered ruthenate, $H_{0.2}RuO_2{\cdot}0.5H_2O$, consisting of regularly stacked slabs of RuO_6 octahedra and interlayer proton and water. Heating this under 5% H_2 + 95% N_2 gas at 200 °C yielded powder with a metallic luster. Figure 1a shows the powder X-ray diffraction (XRD) pattern after reduction of a layered ruthenate. The observed peaks were successfully attributable to a single phase of bulk ruthenium metal, suggesting that the layered ruthenate was completely reduced. Scanning electron microscopy (SEM) observation of the obtained ruthenium metal displays layered morphology, which may be inherited from the morphology of the

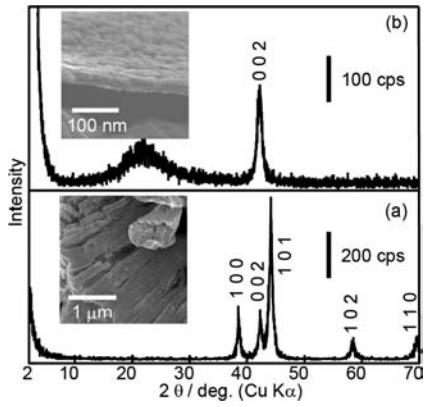

Figure 1. XRD patterns for metallized products obtained from (a) a layered precursor and (b) a restacked film of the RuO_2 nanosheets. Insets: their SEM images.

Received: December 10, 2012
Published: February 19, 2013

   dx.doi.org/10.1021/ic302720d | *Inorg. Chem.* 2013, 52, 2280−2282

layered ruthenate. A weight loss up to 500 °C (see Figure S1 in the Supporting Information, SI) revealed that its metallization began to occur at ~115 °C, which seems to be comparable to that of rutile-type RuO_2 nanoparticles, above 100 °C.[7c]

Next, the reduction of a thin film composed of restacked nanosheets, which was obtained by drying a droplet of the exfoliated nanosheet suspension on the silicon substrate,[8] was conducted. XRD analysis of an as-deposited film exhibited a series of strong diffraction peaks typical of lamellar ordering with d = 1.65 nm (not shown), indicating reconstruction of a layered structure composed of RuO_2 slabs interleaved with hydrated tetrabutylammonium ions. After treatment with 5% H_2 + 95% N_2 gas at 200 °C, a metallic film exhibiting only one diffraction peak assignable to 002 of the ruthenium metal (Figure 1b) was formed. This indicates that the ruthenium film has a strong c-axis orientation, despite the use of an amorphous substrate. SEM images show that the lamellar morphology is preserved with a thickness of several hundred nanometers.

The above results suggest that a topotactic reduction to ruthenium metal occurred; in other words, the atomic arrangement in the RuO_2 nanosheet slabs is preserved in the reduced metallic ruthenium. What transition would occur in the extreme case of a single nanosheet as an ultimately thin reactant? A self-assembled monolayer film of which the RuO_2 nanosheets lay flat to SiO_2 glass substrate was used for this case. The in-plane XRD pattern of the as-deposited monolayer film exhibited at least two diffraction peaks assignable to 10 and 11 of a 2D hexagonal cell having a = 0.2929(6) nm (see Figure 2a). After reduction at 200

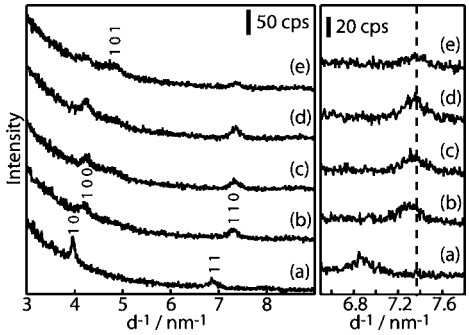

Figure 2. In-plane XRD patterns for (a) an as-grown monolayer film and that heated at (b) 200, (c) 300, (d) 400, and (e) 500 °C.

°C, two peaks that were shift to a larger $1/d$ region were observed. Judging from the metallization behavior of the bulk systems, the two XRD peaks can be indexed as 100 and 110 of hcp-Ru. The lack of indexes associated with 00l in the in-plane direction can be explained by the formation of ruthenium metal having a preferential orientation with the c axis perpendicular to the substrate, consistent with the result observed in the restacked film of the nanosheets. Upon an increase in the reduction temperature, a gradual surge of a small peak at 4.7 nm^{-1} is evident. This peak is assignable to 101 of ruthenium metal, which is the strongest reflection in polycrystalline ruthenium. Heat treatment above 300 °C induces a rearrangement of the Ru atoms via thermal diffusion, consequently leading to a collapse of the c-axis orientation.

The topographical change before and after metallization was examined by tapping-mode atomic force microscopy (AFM; see Figure 3). As-deposited nanosheets are visualized as lamellar objects with a thickness of about 1.2 nm and a lateral size ranging from submicrometer to micrometer. The majority of the RuO_2

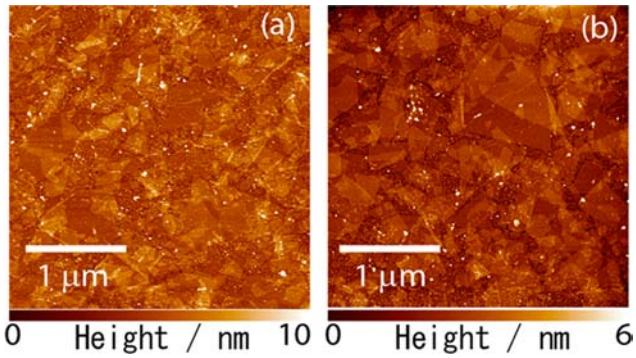

Figure 3. AFM images of an as-grown film of RuO_2 nanosheets (a) and its heated product (b).

nanosheets were adsorbed on the substrate as a monolayer state, although some gaps between the nanosheets and overlapping were inevitable under the present fabrication recipe. Interestingly, the nanosheet morphology remained nearly unchanged after metallization. The results strongly suggest that a topotactic conversion from RuO_2 to ruthenium metal nanosheets occurs. The average thickness of ~0.6 nm acquired from the AFM images for the ruthenium metal nanosheets is much smaller than those of conventional oxide-type nanosheets (see Figure S2 in the SI). This thickness can only be rationalized by a release of O atoms from the RuO_2 nanosheets. Furthermore, coverage analysis based on the height histogram of Figure 3a,b presents only a faint decrement in coverage (from ~90% to ~85%). The slight shrinkage coincides with the change in the in-plane periodic structure from 0.29 to 0.27 nm, about 7% shrinkage. This excellent agreement in the structural feature is concrete evidence that topotactic metallization took place.

A previous study with $Ti_{0.91}O_2$ nanosheets revealed that the structural transformation is affected by the stacking number of the nanosheet layers because thermal diffusion is a decisive factor in the ultrathin reactant.[5] Hence, investigating the transition behavior of the multilayered RuO_2 nanosheets should be of great help in understanding topotactic metallization of the RuO_2 nanosheet monolayer. In-plane XRD analysis revealed that reduction leads to polycrystalline-like ruthenium metals with no preferential orientation (see Figure S3 in the SI), similar to the case for reduction of layered $H_{0.2}RuO_2 \cdot 0.5H_2O$. Consequently, topotactic metallization is believed to be peculiar to nanoscopic systems such as the monolayer RuO_2 nanosheet.

$I-V$ measurement of these samples using a four-probe system shows unusual behavior of sheet resistance. The as-deposited monolayer film of the RuO_2 nanosheets exhibited a sheet resistance of 4×10^6 Ω/square. The sheet resistance of the as-deposited RuO_2 nanosheet film is inversely proportional to the deposition number of the nanosheet layer (see Figure S4 in the SI), which is similar to the case of our previous work on the self-assembled film of $RuO_{2.1}$ nanosheets.[10] Surprisingly, reducing the monolayer RuO_2 nanosheet yielded a black film, which showed poor electronic conduction. The sheet resistance of the nanosheet films has a strong dependence on the in-plane network of the nanosheets, i.e., the amount of overlapping.[10] Because the present self-assembled films had adequate coverage of the adsorbed nanosheets, the shrinkage of the sheet size after metallization may have decreased the amount of overlapped portion of the nanosheets, which, in turn, may have affected measurement of the sheet resistance. On the other hand, the multilayered ruthenium metal films exhibited sheet resistance

dx.doi.org/10.1021/ic302720d | Inorg. Chem. 2013, 52, 2280−2282

that was lower than that of the original RuO_2 nanosheet films. On the basis of the crystallographic thickness, the resistivity of the obtained ruthenium metal film was calculated. Assuming that the ruthenium metal film acquired from the six-layered sample has a thickness of 1.2 nm, its resistivity can be estimated as approximately 9×10^{-5} Ω cm, comparable to that of a ruthenium single crystal. This indicates that the formation of a metallic bond, i.e., the generation of free electrons, can be attained in multilayers.

There is a large difference in the reduction behavior between the monolayer and multilayer reactants. This is supported by a broad IR absorption band associated with metallic nature, as shown in Figure 4. The monolayer sample exhibited a negligible

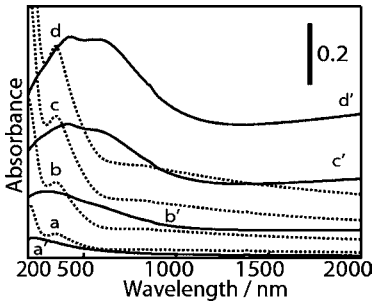

Figure 4. UV−vis−IR absorption spectra for layer-by-layer nanosheet films having layer numbers of (a and a′) 1, (b and b′) 3, (c and c′) 6, and (d and d′) 10 before (broken line) and after (solid line) reduction.

absorption band in the IR range after heating, meaning a poor conductivity. As for the multilayers, the resultant ruthenium metal films have distinctive absorption bands in the IR range, and the absorbance is highly dependent on the number of layers. The enhancement of the electronic conductivity observed in the multilayers may be explained by the construction of a unit cell of a *c*-axis-oriented ruthenium metal composed of three layers of Ru atoms in a close-packed hexagonal lattice. A further study on these ruthenium nanometals is now underway particularly from a theoretical point of view.

In conclusion, we have found, for the first time, topotactic metallization of the oxide-type nanosheets. The finding revealed in this study can be considered as a novel phenomenon peculiar to a two-dimensionally bound nanoscopic system. Because the initial layer number of the RuO_2 nanosheets governs the formation of the resulting metallic bonds, this would be of special interest not only for fundamental metal science but also for application toward conductive or catalytic material synthesis. Similar structural conversions are expected to be discovered in other nanosheet systems.

■ ASSOCIATED CONTENT

Ⓢ Supporting Information

Experimental procedures, thermogravimetric analysis data, an AFM image, in-plane XRD patterns, and sheet resistances. This material is available free of charge via the Internet at http://pubs.acs.org.

■ AUTHOR INFORMATION

Corresponding Author

*E-mail: wsugi@shinshu-u.ac.jp (W.S.), K_F@aug.rikadai.jp (K.F.). Fax: +81-268-21-5452.

Notes

The authors declare no competing financial interest.

■ ACKNOWLEDGMENTS

This work was supported by CREST of JST and by a Grant-in-Aid for Young Scientists (B) of JSPS. The in-plane XRD measurements were performed with the approval of the Photon Factory Program Advisory Committee (2011G003).

■ REFERENCES

(1) Kumar, C. S. S. R., Ed. *Metallic Nanomaterials*; Wiley-VCH Verlag GmbH & Co. KGaA: Weinheim, Germany, 2009.

(2) (a) Walker, G. F. *Nature* **1960**, *187*, 312. (b) Nadeau, P. H.; Wilson, M. J.; McHardy, W. J.; Tait, J. M. *Science* **1984**, *225*, 923.

(3) (a) Treacy, M. M.; Rice, S. B.; Jacobson, A. J.; Lewandowski, J. T. *Chem. Mater.* **1990**, *2*, 279. (b) Sasaki, T.; Watanabe, M.; Hashizume, H.; Yamada, H.; Nakazawa, H. *J. Am. Chem. Soc.* **1996**, *118*, 8329. (c) Liu, Z.-H.; Ooi, K.; Kanoh, H.; Tang, W.-P.; Tomida, T. *Langmuir* **2000**, *16*, 4154.

(4) (a) Novoselov, K. S.; Geim, A. K.; Morozov, S. V.; Jiang, D.; Zhang, Y.; Dubonos, S. V.; Grigorieva, I. V.; Firsov, A. A. *Science* **2004**, *306*, 666. (b) Stankovich, S.; Dikin, D. A.; Dommett, G. H. B.; Kohlhaas, K. M.; Zimney, E. J.; Stach, E. A.; Piner, R. D.; Nguyen, S. T.; Ruoff, R. S. *Nature* **2006**, *442*, 282.

(5) Fukuda, K.; Ebina, Y.; Shibata, T.; Aizawa, T.; Nakai, I.; Sasaki, T. *J. Am. Chem. Soc.* **2007**, *129*, 202.

(6) (a) Ryden, W. D.; Lawson, A. W. *Phys. Rev. B* **1970**, *1*, 1494. (b) Trasatti, S. *Electrochim. Acta* **1991**, *36*, 225.

(7) (a) Matsui, Y.; Hiratani, S.; Kimura, S. *J. Mater. Sci.* **2000**, *35*, 4093. (b) Jelenkovic, E. V.; Tong, K. Y.; Cheung, W. Y.; Wong, S. P. *Microelectron. Reliab.* **2003**, *43*, 49. (c) Prudenziati, M.; Morten, B.; Travan, E. *Mater. Sci. Eng.* **2003**, *B98*, 167.

(8) Fukuda, K.; Saida, T.; Sato, J.; Yonezawa, M.; Takasu, Y.; Sugimoto, W. *Inorg. Chem.* **2010**, *49*, 4391.

(9) Powell, R. W.; Tye, R. P.; Woodman, M. J. *Platinum Met. Rev.* **1962**, *6*, 138.

(10) Sato, J.; Kato, H.; Kimura, M.; Fukuda, K.; Sugimoto, W. *Langmuir* **2010**, *26*, 18049.